# ELECTRON SPIN RESONANCE STUDY OF H CENTERS IN $RbCaF_3$

By

Rick Alan Burris

Bachelor of Science

Oklahoma State University

Stillwater, Oklahoma

1976

Submitted to the Faculty of the
Graduate College of the
Oklahoma State University
in partial fulfillment of
the requirements for
the Degree of
Master of Science
May, 1978

ELECTRON SPIN RESONANCE STUDY OF

H CENTERS IN $RbCaF_3$

THESIS APPROVED:

Larry E. Halliburton
Thesis Adviser

W. A. Sibley

Norman N. Durham
Dean of Graduate College

## ACKNOWLEDGMENTS

Behind every pursuer of higher aspirations, it is said that one will find a group of people who showed sufficient interest in the endeavor to encourage its completion. In the instance of this author's work, this interest came in the form of the affection of his family, relatives, and friends. It also came in the form of a fortuitous string of competent and concerned instructors, from the first enthusiastic encounter with an eighth grade algebra teacher to the returned enthusiasm and expertise of Dr. P. A. Westhaus, undoubtedly the best instructor the author has ever encountered in physics. The person that did the most to encourage continuation of the pursuit of physics was Dr. Larry E. Halliburton, who also showed what it means to be a professional and the responsibilities thereof.

Financial support through a Research Assistantship in conjunction with the Radiation Safety Program under the very understanding supervision of Dr. Elton E. Kohnke is greatly appreciated. Dr. Kohnke also provided assistance in many areas, in and out of physics, for which the author is grateful.

Besides these outstanding individuals, the author is grateful to the many more whose invaluable aid cleared the path to his success.

TABLE OF CONTENTS

## LIST OF TABLES

## LIST OF FIGURES

# CHAPTER I

## INTRODUCTION

The study of radiation-induced defects in solids started before 1900 with limited success. Not until the age of technology was well underway could the study truly come into its own with the help of the technological advances of the second world war. With the war also came the urgent need to study radiation-induced defects. Later, these defects came to be studied for peaceful purposes, and the recent consciousness of the energy situation has spurred these investigations still more.

Solids in general are too complex to do microscopic analysis of radiation defects. The logical starting point for such an investigation would be perfect (or as close as possible) crystals. The radiation defects in alkali halides, such as LiF, KCl, and NaCl, were first to be characterized. The study then expanded to the more complex materials such as the perovskite-structured fluorides ($NaMgF_3$, $KMgF_3$) and simple oxides (BeO, MgO, and SrO).

Electron spin resonance (ESR) has been used successfully since the early 1950's to obtain detailed information about well-localized defect centers (called point defects)

in simple crystalline solids. Two general types of point defects were found to occur frequently in halide materials: (A) the electronic defect, or V-type center[1], first characterized by Castner and Kanzig (2) in 1957 using LiF; and (B) the ionic defects, interstitial atoms and vacancies, or H- and F-type centers, respectively, first characterized by Kanzig and Woodruff (3). These ionic defects come in pairs, known as Frenkel pairs, of interstitials (H centers) and lattice vacancies (F centers). The H center was found by Kanzig and Woodruff to be a halogen$_2^-$ molecule-ion centered on a halide lattice site, which would imply Frenkel pair defects. This has also been studied in a perovskite-structured fluoride--$KMgF_3$ (4).

There are two known processes that produce ionic defects--elastic collision and radiolysis. The elastic collision process has been found to be the dominant damage process in the simple oxides, such as MgO (5). Radiolysis, however, presents a more tenable method for interstitial production in halide materials, since ionic displacement is easily achieved with relatively low energy electrons as well as X and gamma rays. A study by Riley and Sibley (6) supports this "photochemical" radiation-damage process for the production of ionic defects in $KMgF_3$, and ionic damage is even more easily obtained in $RbCaF_3$. H center production in $RbCaF_3$ is then tentatively assigned to radiolysis.

---

[1]See Sonder and Sibley (1), for the notation used.

It is the purpose of this paper to study the H center in $RbCaF_3$. Several properties of this defect have turned out to be non-standard and have led to some interesting questions. First, some background information is necessary and is presented in the remaining two sections of this chapter. The crystal's structure, phase changes, and previously studied defects are outlined in the first section. The second section provides a short summary of work on a few other perovskite-structured fluorides for later comparison to the results of this investigation.

## A. The $RbCaF_3$ Crystal Structure

The room temperature structure of $RbCaF_3$ is the cubic perovskite as shown in the ball-and-stick model in Figure 1. The lattice parameter is from Wyckoff (7). As in most other materials of its kind, $RbCaF_3$ goes through phase changes. Three of them have been reported (8) at 198 K, 42 K, and 7 K from specific heat measurements.

The optical birefringence, Raman scattering, and neutron scattering measurements of Bates, Major and Modine (9) show the 198 K transition to be second order with a small first order contribution, and give indication of a small (0.15 K) hysteresis. Halliburton and Sonder (10) in their ESR investigation of the $V_K$ center found that this defect, an intrinsic self-trapped hole shared by two adjacent fluorine ions, was rotated off the [110] direction by 7.1° at 77

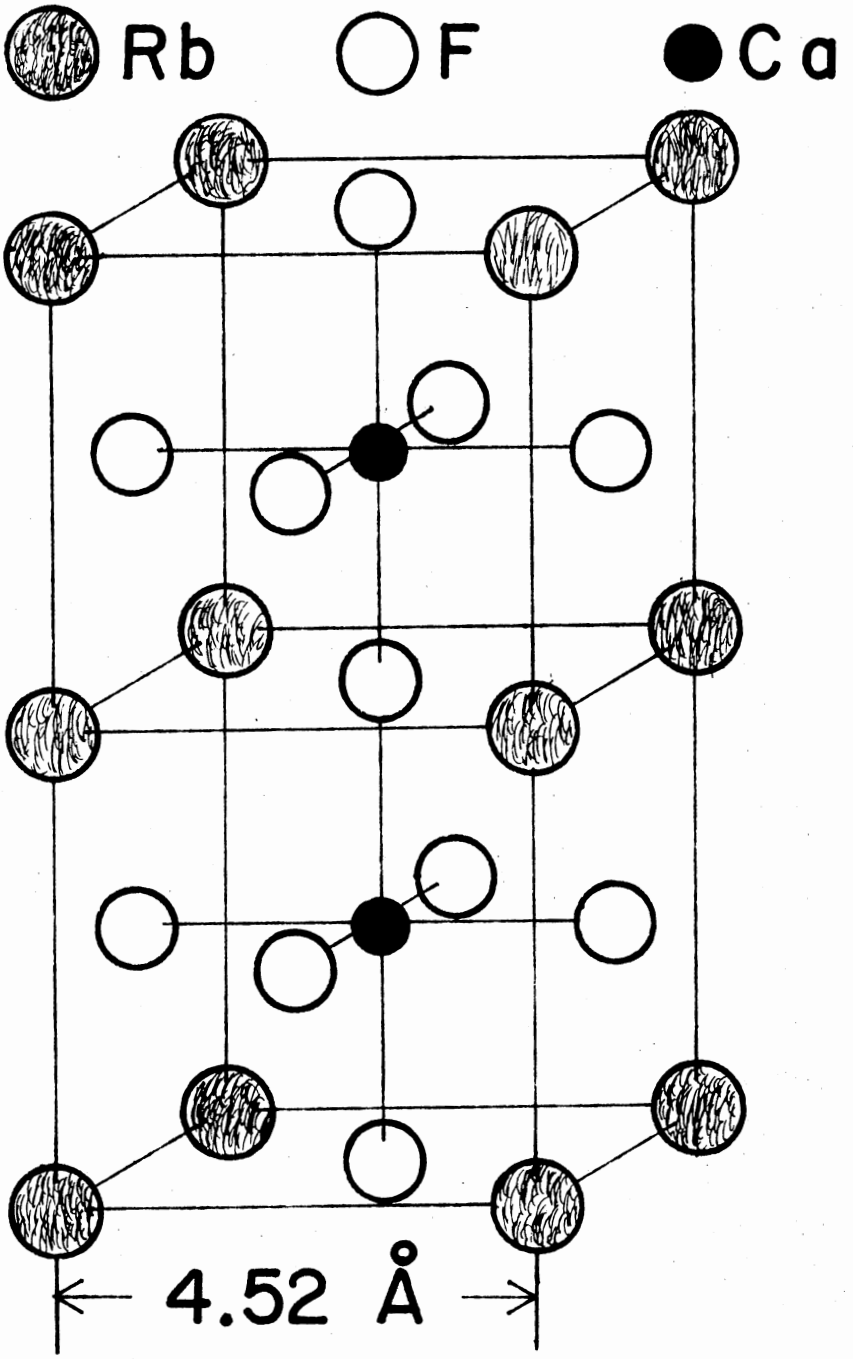


Figure 1. The Crystal Structure of RbCaF

K. This suggests a rotation of the normal $CaF_6$ octahedra by this same magnitude about a [100]-type direction. Modine, Sonder and Unruh (11) in their original study of the material, observed domain structure in the tetragonal phase in their ESR and birefringence measurements. These domains aligned themselves in the three [100] directions with preferential alignment most noticeable in crystals that had not been taken through the phase changes very many times and had been annealed at about 350° C for several hours. The aligned domains also occurred in crystals cut in thin plates. Seretlo, Martin and Sonder (12) have studied the optical spectra of $RbCaF_3$ in the tetragonal phase and at liquid helium temperature, but could make no definite assignments of the optical bands.

The second transition at 42 K is of lower order than the first transition. This phase reportedly requires either a virgin sample (one that has not been previously cooled below 40 K and warmed to room temperature) or it requires that the crystal first be annealed at 350° C for several hours. Thus far, there has been no study of the lattice structure in this phase. Bates et al. reevaluated the hysteresis reported by Modine et al. and showed that this transition occurred at varying rates between 42 K and about 25 K. They then used Raman scattering data to show that both phases can be present in this temperature range. They could not, however, observe either this transition or the one at 7 K with neutron scattering.

The third transition (as well as the first two) has been definitely established at 7 K by Ko and Unruh (8) in specific heat experiments, but the change in specific heat was too small to say much more about the transition. No information is available on the structure of this phase.

## B. Other Perovskite-Structured Fluorides

Of the 125 possible combinations of the IA, IIA, and VIIA chemical groups of the form $RMX_3$, only 10 are reported in Wyckoff (7) and only six of these are assigned to the cubic perovskite structure. In this section we will briefly describe four of these materials: $NaMgF_3$, $KCaF_3$, $KMgF_3$, and $RbMgF_3$.

The first crystal, $NaMgF_3$, is not a cubic perovskite below 900°±25° C. From 760° to 900° C it is tetragonal, and below 760° C it is orthorhombic. At room temperature, its structure can best be described as perovskite with the octahedra "tilted" twice--once about a tetrad axis as in $RbCaF_3$ at low temperatures, and once again about a diad axis. This unique double tilt makes it possible to obtain a [100]-type $V_K$ defect, studied by M. Young for his dissertation (13), between two fluorines of seperate octahedra. The usual [110]-type $V_K$ were also studied, but since the symmetry of the material is so low, the detailed study of both $V_K$ types was severely hampered. To date, no interstitials have

been studied in this material since its low symmetry makes the detailed study of its defects quite difficult. Optical studies (12) show, however, that F and F-aggregate centers exist in $NaMgF_3$ so that H centers are very likely to occur as well.

$KCaF_3$ has been studied very little since 1960. No information is available on its point defects and little information is available on its structure. Wyckoff (7) calls its structure perovskite with a monoclinic distortion. Since this material is closely related to $KMgF_3$ as well as $RbCaF_3$, a study of its defects may provide more insights into the nature of the defects and phase changes in these simple crystals.

For many years, researchers have investigated magnetic $KMnF_3$, and for almost as many, they have looked at its close relative $KMgF_3$. Intrinsic (H) and impurity-associated ($H_A$) interstitial defects have been studied in $KMgF_3$ (4, 16). The intrinsic H center was found to be somewhat analogous to that in KCl--the interstitial pair of flourines interacted slightly with another pair on either side along the [110] axis, as shown in Figure 2(A), taken from Rose (4). Since $KMgF_3$ is a cubic perovskite, there are close-packed rows of fluorines which would make it possible for a replacement collision sequence to occur in the radiolysis process. As will be discussed later, there is some evidence that this collision sequence may not be necessary. The impurity-asso-

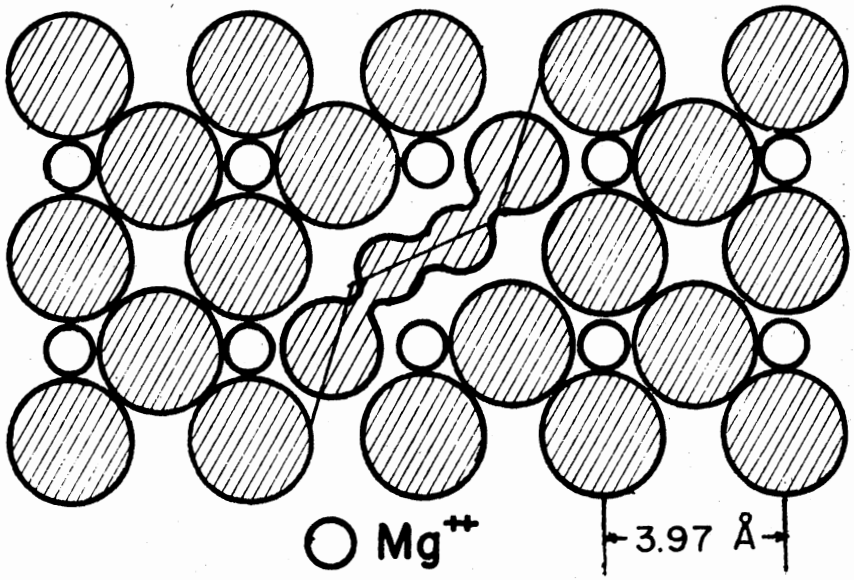


(A)

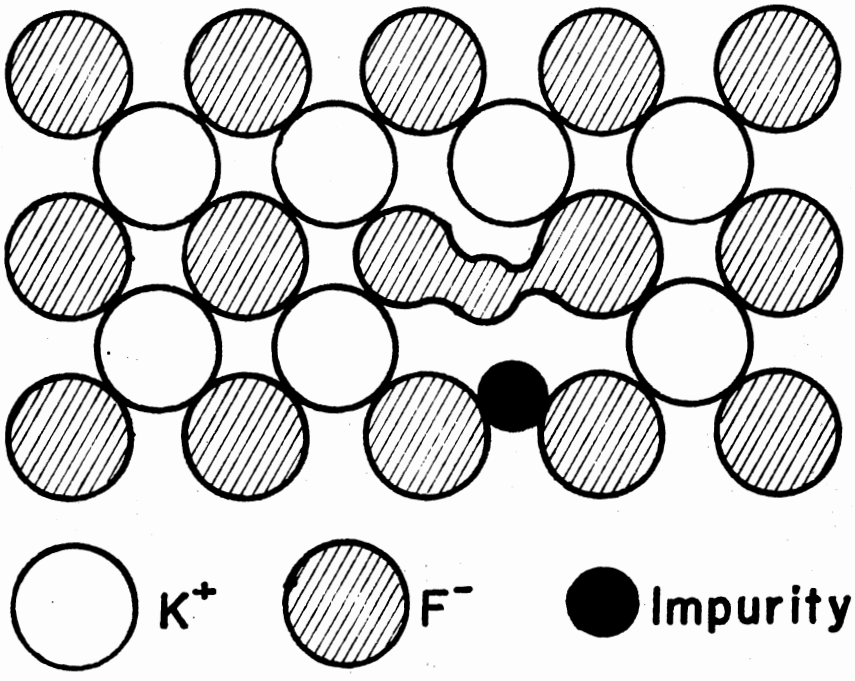


(B)

Figure 2. The (A) H and (B) $H_A$ Center Models in $KMgF_3$

ciated H center was found to be only three interacting flourines along a bent bond (16). The unique discovery about this latter center was that the interstitial displayed restricted motion between the two end flourines. This motion averaged out the ESR spectra at liquid nitrogen temperature, but was inhibited at liquid helium temperature. The model is shown in Figure 2(B).

The final "perovskite" crystal, $RbMgF_3$, turns out not to be perovskite. Recent optical studies by Koumvakalis and Sibley (14) have confirmed that this material has a hexagonal symmetry, similar to the hexagonal form of $BaTiO_3$. Their study revealed some of the properties of the F and F-aggregate centers and the $V_K$ center. ESR studies of the $V_K$ center have recently been done at this institution by Saha (15), but have not yet been published. To date, no studies have been made of the H center in $RbMgF_3$.

Table I summarizes the crystal symmetries, lattice constants, defect types studied by ESR, and spin Hamiltonian parameters for these four materials. The crystal symmetries are given as "C" for cubic, "T" for tetrahedral, "O" for orthorhombic, and "H" for hexagonal. The lattice parameters are the approximate c-axis distance between alkali atoms, given in angstrom units. References are given for each defect. The spin resonance parameters in the table are representative values only. Where the defect involves more than one nucleus, average values are given unless the values

differ widely, in which case both values are given. All nuclear hyperfine terms are given in Gauss. A question mark means no information is available.

TABLE I

A SUMMARY OF THE RESULTS OF PREVIOUS WORK

| MATERIAL | SYMMETRY | C | DEFECTS | PARAMETERS |
|---|---|---|---|---|
| $NaMgF_3$ | C,T,O | 3.826 | [100] $V_K$ (13) | gz=2.0034<br>Az=928 |
| | | | [110] $V_K$ (13) | gx,y~2.02<br>gz=2.004<br>Ax,y~35<br>Az~903 |
| $KCaF_3$ | C? | 4.371 | ? | ? |
| $KMgF_3$ | C | 3.973 | $V_K$ (17) | gx,y~2.020<br>Gz~2.0024<br>Ax,y~56.7<br>Az~883.6 |
| | | | H(4) | gx,y~2.013<br>Gz=2.0032<br>Ax,y~0<br>Az~955 |
| | | | $H_A$ (16) | gx,y~2.02<br>Gz=2.0018<br>A1x,y~187<br>A1z=1113.8<br>A2x,y~67<br>A2z=599.6<br>A3x,y=5.4±4.<br>A3z=50.7 |
| $RbMgF_3$ | H | 4.09 | $V_K$ (15) | gx,y~2.021<br>Gz=2.002<br>Ax,y~100<br>Az=866 |

# CHAPTER II

## EXPERIMENTAL PROCEDURE

This chapter outlines the general experimental procedure and equipment used in obtaining the preliminary characteristics and data for the H center in $RbCaF_3$. Section A describes the sample crystals and section B describes the apparatus and procedure.

### A. Sample Preparation

The crystals used in these experiments were obtained from Dr. E. Sonder at the Oak Ridge National Laboratories and are from the same batch as those used in the paper by Modine et al. (11). They were prepared by a Bridgman technique from RbF and $CaF_2$ of stated >99.9% purity. One crystal used in this study measured 3X3X6 mm, and the rest were of comparable size, although flattened somewhat in the first dimension.

A list of the major impurities in the crystals and their approximate concentration is reproduced from the paper of Modine et al. in Table II.

TABLE II

MAJOR IMPURITIES IN $RbCaF_3$ CRYSTALS

| Impurity | Concentration (PPM) |
|---|---|
| Al | 100 |
| Fe | 10 |
| K | 1000 |
| Mg | 20 |
| Na | 100 |
| Cs | 100 |

## B. The Procedure

The initial production of defects made use of the electron beam output of a Van de Graaff accelerator. One trial irradiation was done at room temperature with no usable results and the rest of the irradiations were done at liquid nitrogen temperature with the sample placed in a styrofoam cup. The cup, with the sample broadside against the wall, was placed behind a 3 mm-thick aluminum safety barrier which was, in turn, 4 cm from the 0.2 mm aluminum window on the accelerator. This arrangement resulted in a total distance between the sample and accelerator window of 6 cm. Except for a few exploratory experiments, the irradiations were done at 1.5 MeV and 10 microamperes. The styrofoam cups and the liquid nitrogen were changed after every 5 minutes of irradiation time.

Two methods were used to bleach the samples with ultraviolet light while at liquid nitrogen temperature. One method was to bleach it while in the cavity through slits in the cavity wall. This method was used when the variable temperature assembly was being used, or when the alignment of the crystal was critical. Another method, if the finger Dewar was being used, was to remove the Dewar from the cavity, set it in a ring stand, and bleach the crystal while in the Dewar. The ultraviolet light was supplied in both cases by an unfiltered 100 watt mercury arc lamp.

The ESR spectra were obtained with an X-band homodyne spectrometer as illustrated in the block diagram in Figure 3. The magnetic field was supplied by a current-regulated, 6-inch Varian electromagnet. The field was modulated at 100 kHz using the power output of the Varian lock-in detector connected to modulation coils just outside the cavity walls. Field measurements were made with an NMR proton probe, a PAR lock-in detector, and a Hewlett-Packard digital frequency counter.

A frequency stabilized klystron supplied the microwave power. The ESR signal, modulated by the 100 kHz field modulation and superimposed on the microwave power reflected from the sample cavity, was recovered with the microwave detector diode. This was then passed through the Varian lock-in detector where the modulation technique allowed the phase sensitive detector to greatly enhance the signal-to-

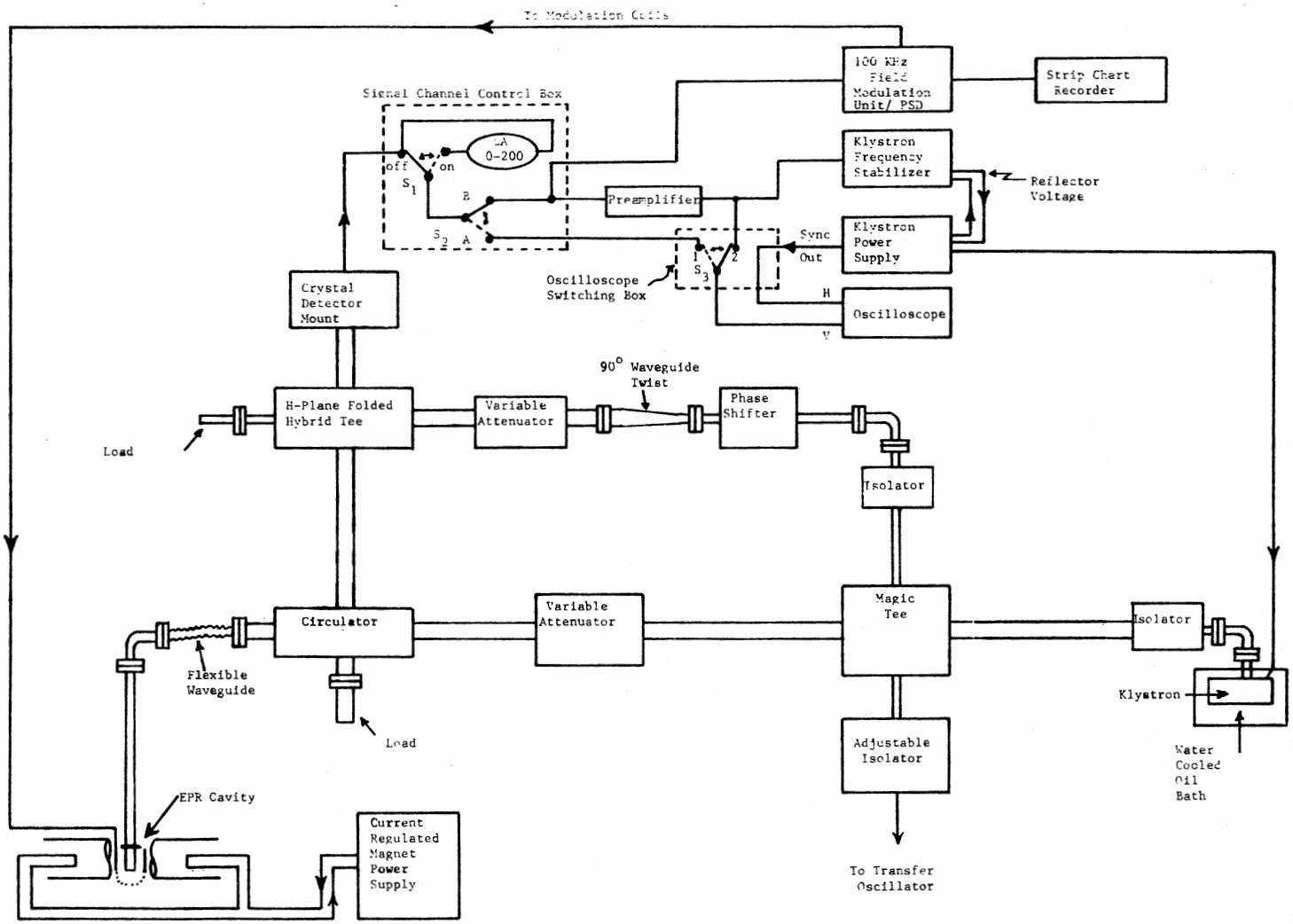


Figure 3. A Block Diagram of the ESR Spectrometer

noise ratio. The resulting first-derivative ESR signal was then displayed on a Leeds and Northrup strip chart recorder. Microwave frequency measurement made use of a Hewlett-Packard transfer oscillator and the RF digital frequency counter.

The cavity used was a Varian V-4531 rectangular ESR cavity which could accommodate either a finger Dewar or the Varian variable temperature assembly. In either case, the sample was mounted in a teflon holder on the end of a hollow stainless steel rod. On the top end of the rod was a cover with angle markings and a pointer, so that the rod and sample could be turned through measurable angles.

The variable temperature assembly was used in the pulsed anneal studies. The temperature was controlled by forcing dry gaseous nitrogen through a heat exchanger immersed in a liquid nitrogen bath, then into a vacuum-sheilded transfer tube with an electric heater inside, and finally through the cavity. The temperature was measured with a copper vs. constantan thermocouple using standard potentiometric techniques. The temperature anneal data were obtained by bringing the sample temperature to the desired level, holding that level for three minutes, then lowering the temperature to near 80 K to take the spectrum.

# CHAPTER III

## EXPERIMENTAL RESULTS

The details of the experimental procedure and results are herein presented in the logical order of discovery--not necessarily in the order of achievement. The results of computer analyses are also presented to complete the identification of the center. The next chapter will discuss some of the implications of this project and will compare these results with those of other materials.

As noted in Chapter I, the octahedra, each composed of one calcium and six fluorine atoms, are rotated by approximately 7° at 77 K as a result of the phase change at 198 K. This produces a unique axis in the crystal which will be referred to as the Z, or [001], crystal axis. Figure 4 shows the [001] spectrum (i. e., the spectrum taken with the magnetic field along the [001] axis) with the line assignments displayed via the stick diagram at the bottom of the figure. The lines assigned to the $V_K$ (self-trapped hole) center have been analyzed by Halliburton and Sonder (10) and were used in these experiments to check the alignment of the sample, since they are more sensitive to the field angle. Notice that the three distinct lines attributed to the H

center (labeled H in Figure 4) have intensities of roughly 1-2-1 relative to each other. The next few paragraphs define a model to explain these lines.

For a free electron (or one that is bound to a nucleus which has no nuclear spin), the spin resonance spectrum is a single line at the magnetic field value given by

$$h\nu = g_{\beta}H$$

where

h = Plank's constant,

$\nu$ = microwave frequency,

g = the electron's Zeeman (g) factor,

$\beta$ = the Bohr magneton,

H = the magnetic field value.

This line corresponds to a transition between the two energy levels for the electron established by the magnetic field. Denoting the spin magnetic moment quantum number by $M_S$ gives, in Dirac's notation

$$|M_S\rangle = E_S\,|M_S\rangle$$

where $E_S$ is the energy eigenvalue due to the spin. The selection for the absorption of microwave energy is $\Delta M_S = \pm 1$, which with two energy levels gives only one spectrum line.

Adding a nucleus with spin 1/2 to the system has the effect of splitting out the spectrum into two lines, implying four energy levels. This can be seen from the quantum mechanical representation

$$|M_S M_I\rangle = E_{SI}\,|M_S M_I\rangle$$

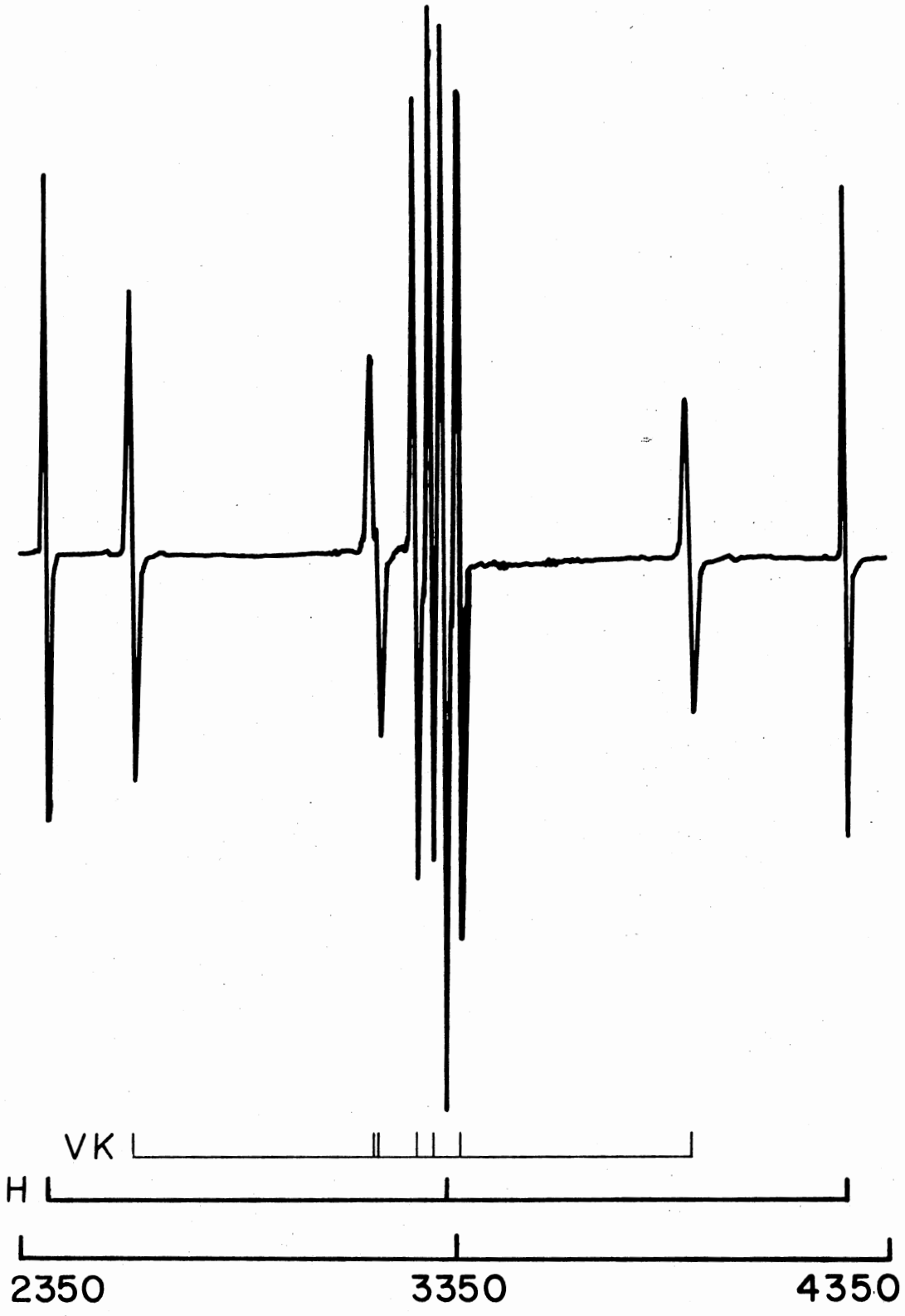


Figure 4. The [001] ESR Spectrum of $RbCaF_3$

where $M_I$ is the nuclear magnetic moment quantum number with the possible values of $\pm 1/2$. Since $M_S$ and $M_I$ are independent and have four distinct combinations, four energy levels result. The selection rule for spin resonance then gives only two lines in the spectrum for this case. Qualitatively, if the difference in magnetic field values of the observed lines is denoted by A, the spectral lines can be described to first order by

$$h\nu = g\beta H + M_I A.$$

For a spin-1 nucleus, with the possible magnetic quantum numbers

$$M_I = 1, 0, -1$$

there are six available energy levels, and three spectral lines result. Notice, however, that all three lines will be equally intense since each transition is equally probable. This, then, could not be the model for the center responsible for the spectrum in Figure 4.

Considering the case of two spin-1/2 nuclei, the number of energy levels is raised to eight. Denoting the first nuclear magnetic quantum number by $M_{I_1}$ and the second by $M_{I_2}$, we have

$$|M_S M_{I_1} M_{I_2}\rangle = E_{SI_1I_2} |M_S M_{I_1} M_{I_2}\rangle.$$

In this case there are eight possible energy states (with the same selection rule) and thus four lines. The lines would follow the condition

$$h\nu = g\beta H + M_{I_1} A_1 + M_{I_2} A_2.$$

If the two A values were equal, then the two central lines corresponding to the cases

$$M_{I_1} = 1/2 \ , \ M_{I_2} = -1/2$$
$$M_{I_1} = -1/2, \ M_{I_2} = 1/2$$

will be degenerate, and the spectrum will again have three lines, but with the central line twice as intense. This, then, is the model that should be used to explain the three lines in Figure 4.

The Hamiltonian used to describe this model is

$$= \beta \vec{S} \cdot \overleftrightarrow{g} \cdot \vec{H} + (\vec{I}_1 + \vec{I}_2) \cdot \overleftrightarrow{A} \cdot \vec{S} - g_N \beta_N (\vec{I}_1 + \vec{I}_2) \cdot \vec{H}.$$

The first term is the electron Zeeman energy and is the largest of the three, giving the value of the magnetic field about which the spectral lines will be (more or less) evenly distributed. The second term is called the nuclear hyperfine term and describes the interaction of the electron with the two nuclei. This term gives the major splitting of the spectral lines. The third term describes the very small perturbation caused by the interaction of the magnetic field with the nuclei. Notice that the two nuclear hyperfine tensors of the two nuclei were taken to be equal (A). This is justified on the basis of the symmetry of the spectrum-there should be only three distinct transition values for the magnetic field aligned with the axis of the model. It can also be seen that the principal axes of the $\overleftrightarrow{g}$ and $\overleftrightarrow{A}$ tensors should be coaxial with the [001] crystal axis. With these restrictions, the model for the center is as pictured in Figure 5.

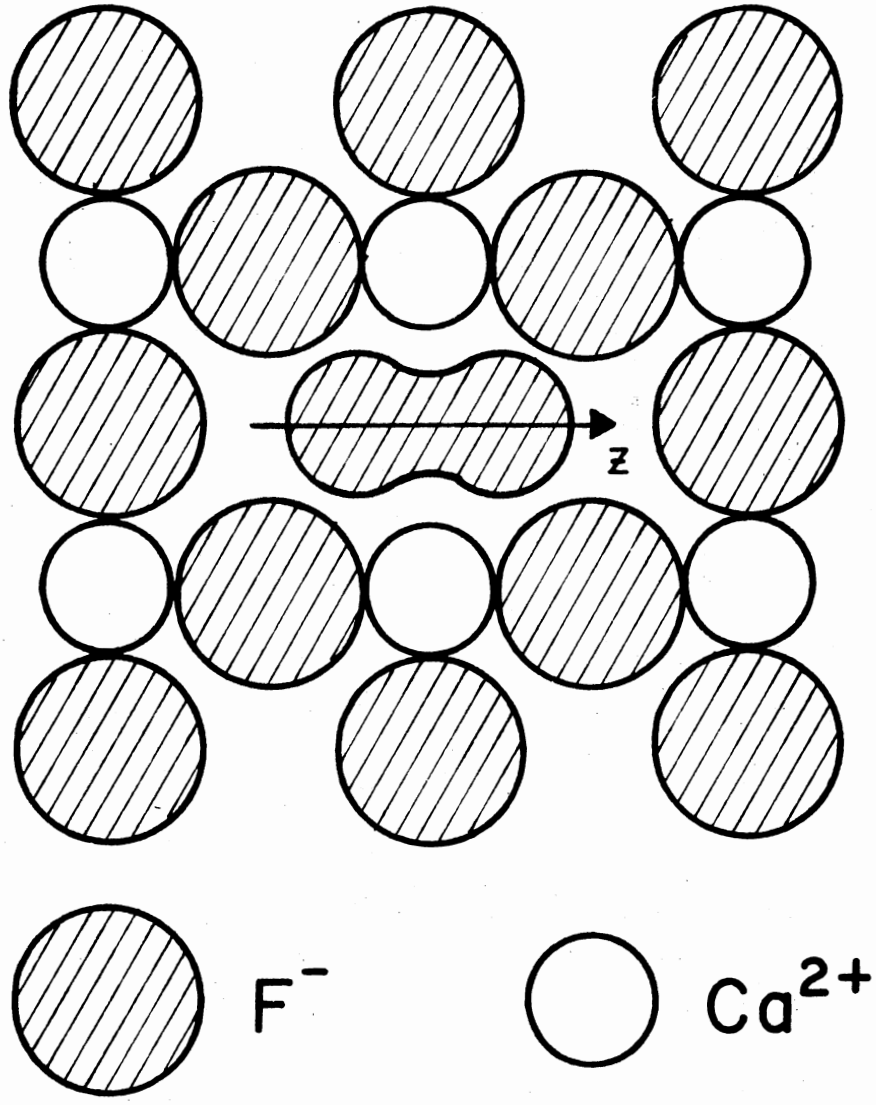


Figure 5. The H Center Model in $RbCaF_3$

Of course, the real physical system isn't as ideal as has been assumed. The [001] spectrum of Figure 4 should also contain lines given by the two other orientations of the center. One would then obtain all the necessary parameters from this [001] spectrum. This is not the case in this instance, however, for reasons to be discussed later. In order to observe the other orientations of the defect, another sample was used. The $V_K$ center spectrum was eliminated in order to measure the field positions of the inner lines. This was done by bleaching the sample with UV light as described in chapter II. After bleaching, three small lines remain on the low-field side of the large central line as shown in Figure 6. These, as well as part of the central line, are due to the centers aligned perpendicular to the [001] axis. Since there are only three, instead of six, of these lines, then the X and Y principal axes of the $\overleftrightarrow{g}$ and $\overleftrightarrow{A}$ tensors are equivalent to within the resolution of the spectrometer. A study of the angular dependence of the spectrum in Figure 7 quickly verifies this[1]. Figure 8 displays the three unique orientations of the defect, with the numbering convention used in the [001] spectra of Figures 4 and 6.

A computer program was used to calculate the g and A parameters by adjusting a given set of parameters to fit the

---

[1]This figure was actually generated by computer from the model, but is representative of an actual experimental study, of which Figure 6 is a part.

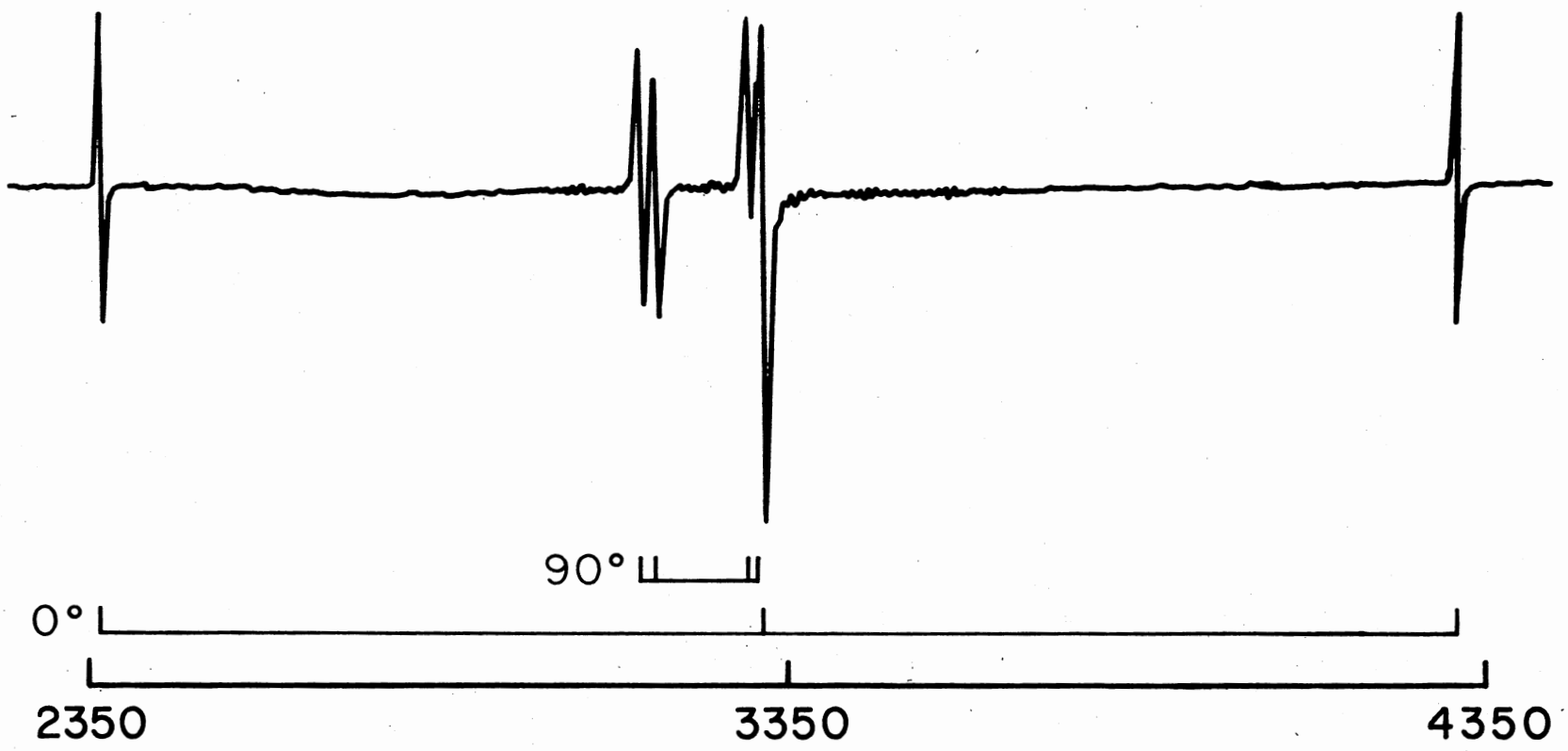


Figure 6. The [001] ESR Spectrum After UV Bleaching

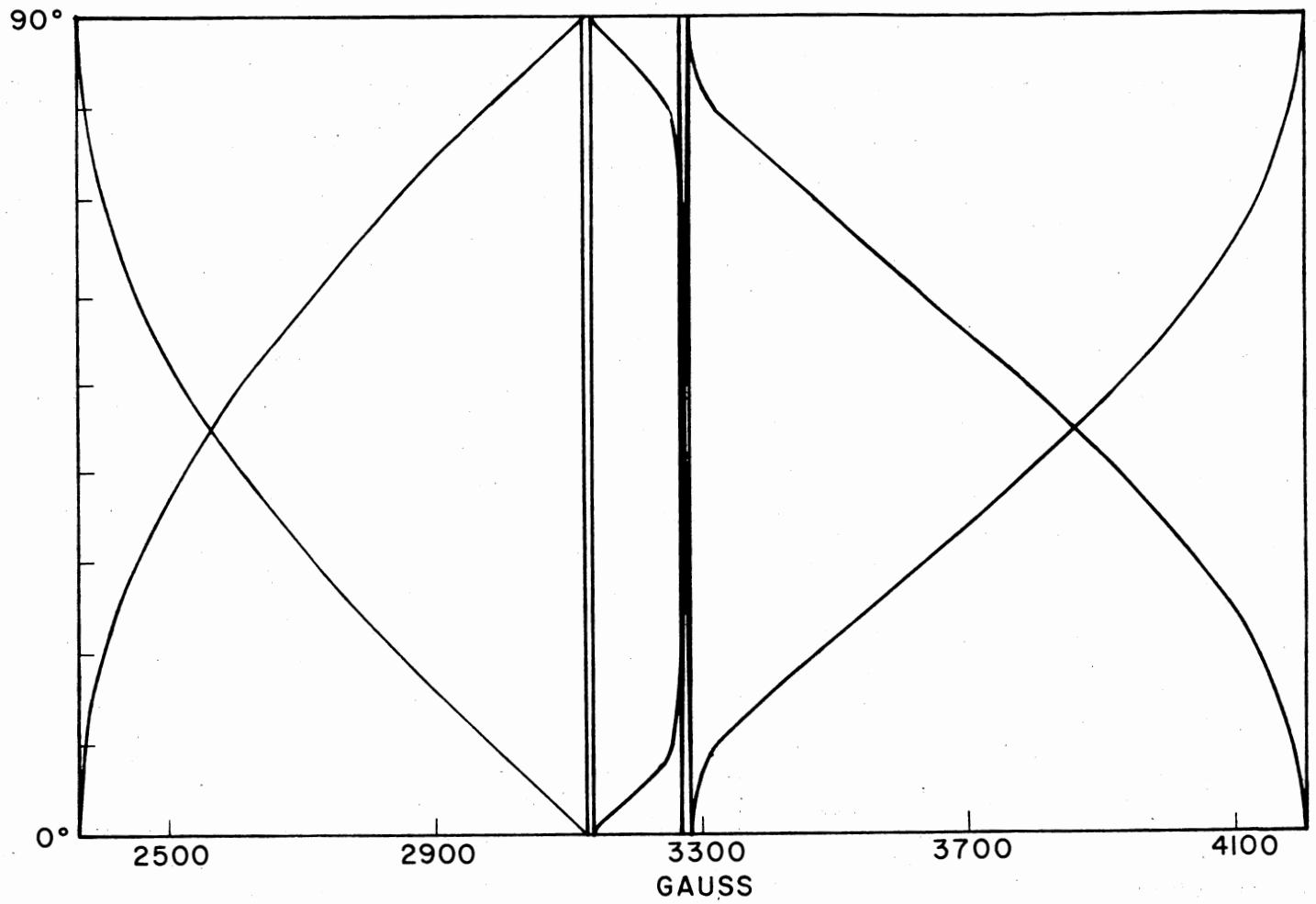


Figure 7. The Angular Dependence of the H Center Spectrum in $RbCaF_3$

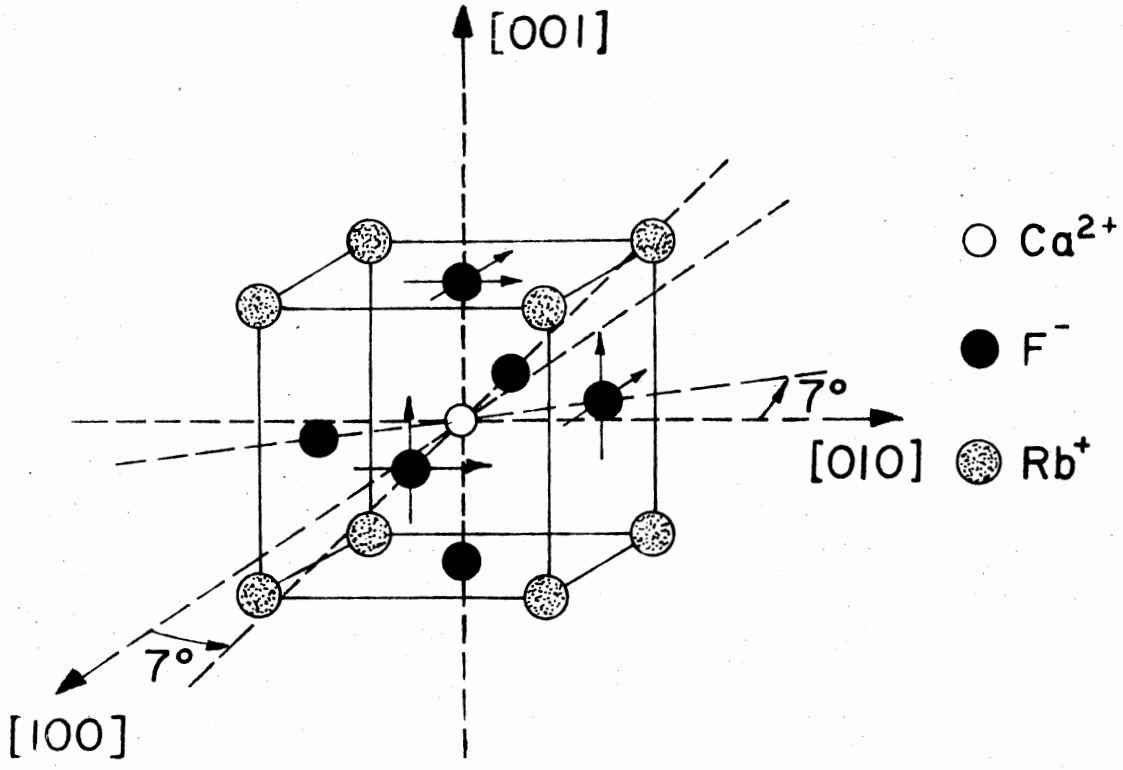


Figure 8. Possible Orientations of the H Center Model in $RbCaF_3$

experimental data. The degree of closeness of the fit was determined by a least-squares process. The lines used were the two outermost lines (giving gz and Az), the two low-field 90° lines (giving gx=gy and Ax=Ay), and the distinct 90° line to the immediate left of the large 0° line (for greater accuracy). The results are given in Table III. The

TABLE III

H CENTER PARAMETERS FROM COMPUTER ANALYSIS

| | | |
|---|---|---|
| gx (=gy) | = | 2.016 |
| gz | = | 2.007 |
| Ax (=Ay) | = | 42.6 G |
| Az | = | 924.3 G |

flowcharts of the programs used are in the Appendix.

The exact nature of the center has still not been completely specified. The model so far consists of two spin-1/2 nuclei aligned along the crystal axis, sharing an electron. The nuclei can be assumed to be fluorines, since they have a nuclear spin of 1/2 and most of the other constituents of the crystal do not. The nuclear hyperfine par-

ameters also compare with the parameters of flucrine nuclei in other defects and materials. More information can be obtained by studying the production of the as yet undefined center in Figure 9. The radiation dosage indicated in the figure is only approximate (18). The $V_K$ are seen to grow and saturate very fast. The center being analyzed is labeled as an H center and grows in much more slowly. This would seem to indicate that this radiation-induced defect is an ionic defect rather than an electronic one. This observation, along with the model developed earlier, indicates that the defect is, indeed, an H center. Since it is an ionic defect it might be assumed to be thermally more stable than the $V_K$ since its destruction requires movement of an atom, rather than the entrapping of an electron. This is not the case, however, as shown in the thermal annealing graph in Figure 10. The $V_K$ and H centers are seen to decay between 110 K and 150 K. This may have caused some confusion in the optical studies of this material, as will be discussed in the next chapter.

A different set of lines from the H and $V_K$ appeared in the spectrum at about 110 K. As the H and the $V_K$ centers decayed, this new line grew until at 160 K it, too, decayed. This center has been tentatively called an $H_A$ center (an H center next to an impurity). Further study is being done on this defect.

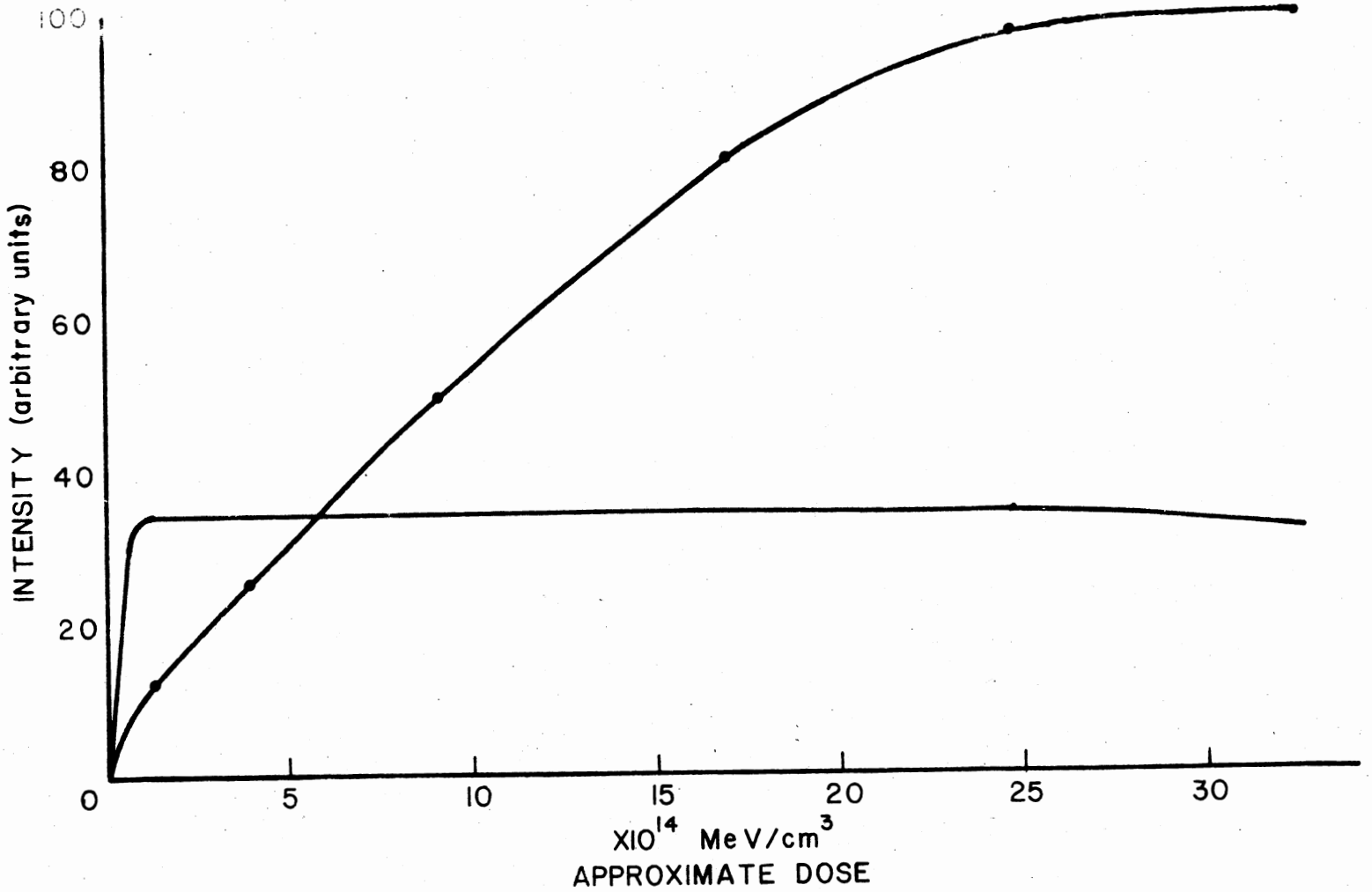


Figure 9. Production Characteristics of the $V_K$ and H Centers in $RbCaF_3$

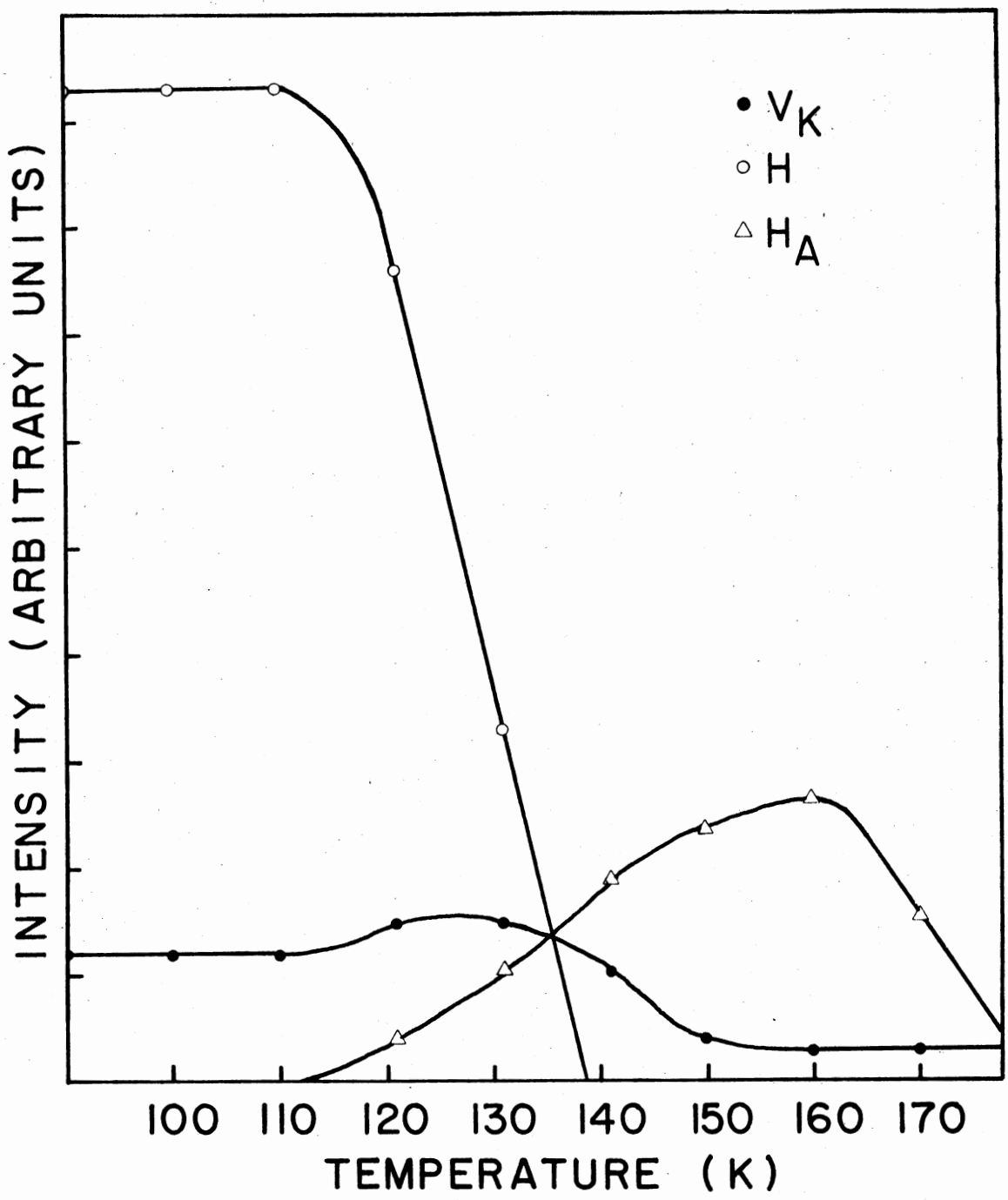


Figure 10. Annealing Characteristics of $V_K$, H, and $H_A$ Centers in $RbCaF_3$

Since the H centers are all aligned with the crystal axis and if equal populations of the three orientations are assumed, it would be expected that the H center spectrum would be the same for the magnetic field oriented along any of the three crystal axes. Figure 11 shows the spectrum of the same sample as in Figure 4 with the magnetic field along a crystal axis perpendicular to the unique [001] axis, say the [100] axis. From the $V_K$ spectra in the two figures, it can be seen that the crystal is largely single-domained. In other words, the $V_K$ spectra, which are sensitive to the rotation of the octahedra, show that most of the octahedra have a common axis of rotation (see Halliburton and Sonder (10)). The criterion for a crystal to be largely singly domained, as outlined in Chapter I, were satisfied for this sample. The sample had not been used very many times previously, and it had been annealed at 360° C for several hours just prior to the experiment. Notice, however, that this was not the case for the spectrum in Figure 6.

The outermost pair of H center lines have greatly diminished in intensity in the [100] spectrum, indicating that the number of centers with their molecular axis (the axis drawn through the two nuclei) parallel to the [100] crystal axis is much less than the number with their molecular axis parallel to the [001] crystal axis. By observing the inner lines during rotation of the magnetic field, one can see that this is also the case for the centers aligned

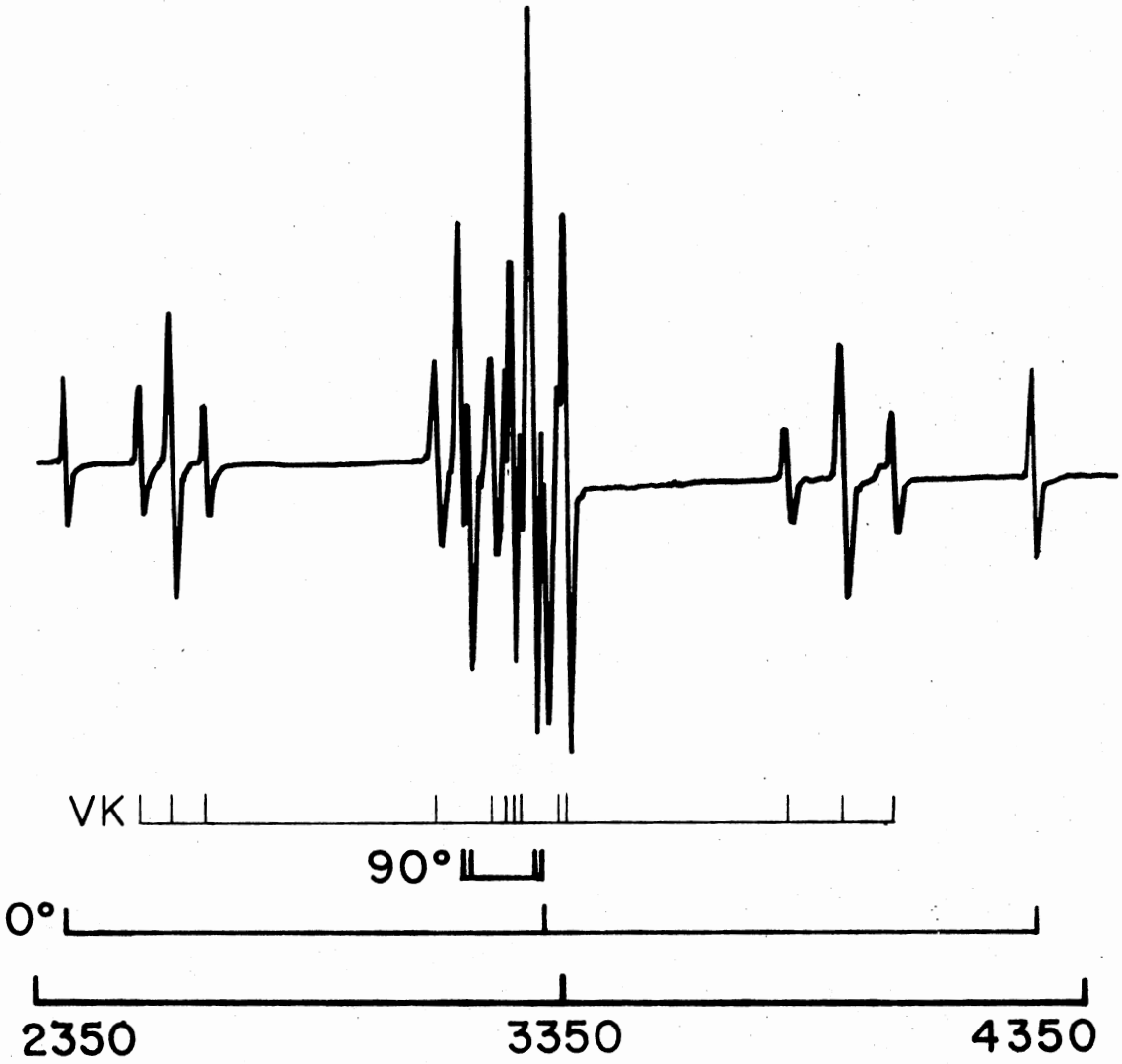


Figure 11. The [100] ESR Spectrum of $RbCaF_3$

with the [010] axis. Thus, the H center in this material is preferentially aligned along the unique axis of the crystal, an effect which is rarely observed in the halides.

In summary, the defect which gives rise to the part of the spectrum in Figure 4 indicated by the 0° markings is an intrinsic H center composed of two fluorine atoms sharing a single fluorine lattice site and an unpaired electron. This defect is preferentially aligned along the unique axis of the crystal. The next chapter will discuss the implications of these results and compare them to those for other halide materials.

# CHAPTER IV

## DISCUSSION AND SUMMARY

The H center in $RbCaF_3$ involves only two fluorine nuclei--it does not interact noticeably with any other anions. This is different from the usual H center encountered in the alkali halides (such as LiF, KCl, and NaCl) and in $KMgF_3$ in that, in these two classes of materials, the two strongly-interacting fluorines also interact to a noticeable extent with two other fluorines along the close-packed row (see figure 2). This can qualitativly be explained through the lattice constants. In $KMgF_3$, the distance between [110] nearest-neighbor fluorines is approximately 2.8 Å and the interaction of the outer two fluorine nuclei with the unpaired electron is very small, as indicated by the nuclear hyperfine interaction tensors for these nuclei (4). In $RbCaF_3$, the distance between [110] nearest-neighbor fluorines is 3.2 Å, so that the interaction should be much less, and in this investigation it was undetectable.

The annealing temperature of the H center in $RbCaF_3$ is also different from the normal. In the Li, Na, and K alkali halides, the H center anneals below liquid nitrogen temperature. The annealing temperature of the H center in $KMgF_3$

has not been definitely established, but it is also below 77 K. The H center in $RbCaF_3$, however, is stable approximately 30 degrees above liquid nitrogen temperature.

Pairing this high thermal stability with the relative ease with which these centers are produced results in the suspicion that the process of replacement collisions along close-packed rows of halides may not be an important part of the radiolysis process in $RbCaF_3$. Since $V_K$ centers (supposedly the initial step in the radiolysis sequence) are at an angle of 7° with the close-pack row axis and the rest of the row zig-zags at a comparable angle, a replacement-collision sequence would require more energy to produce and maintain. Seretlo, Martin, and Sonder (12) mention this in the summary to their paper. Unfortunately, the work presented here cannot lend much support to either prove or disprove this point.

The three optical bands reported for $RbCaF_3$ in the paper of Seretlo et al. can now be identified to a higher degree of certainty. These bands appeared at 320, 400, and 530 nm. Comparing the defect production study of the present investigation to the study given in the paper, it is re-verified that the 530 nm band is due to electron traps.

The 320 nm band, which is produced quickly but doesn't saturate as fast as the 530 nm band, is probably a combination of two spectra--the $V_K$ and the H. The quick initial growth is due to the $V_K$. The gradual rise with further irradiation is due to the growth of the H center.

The 400 nm band whose polarization and narrow width led to suspicions of its origin is most likely the F center. In the case of the H center, it was seen that certain orientations were preferred, showing that the lattice sites for the fluorines are axially symmetric. This could account for a polarization of an F center in that position.

The narrow linewidth of the 400 nm band can be explained by the larger lattice constant. In $KMgF_3$, the ions are much closer together than in $RbCaF_3$. This makes the F center, whose wave function extends over several lattice spacings, more susceptible to thermal broadening of its absorption spectra. The much larger lattice spacing in RbCaF reduces the number of lattice ions within the F center's extent. This in turn reduces the effect of thermal phonons on the F center's absorption, thus narrowing the optical band.

From these assignments, it may be expected that the 400 nm and 320 nm thermal anneal graphs from Seretlo's work should contain slight "steps" in the decay lines in the range of 120 to 180 K. These would be due to differences in the annealing temperature of the H and $H_A$ centers for the 400 nm band, and the $V_K$ and H centers for the 320 nm band. Indeed, a closer look at the 400 nm decay line in Seretlo's paper reveals just such a possibility. Further study is needed to confirm this, however.

Another region requiring further study is the "$H_A$" center. Research is presently under way to determine its structure and verify the nomenclature used for it here. ENDOR could be used, as well, to determine the stabilizing impurity.

The F center in $RbCaF_3$ has not yet been observed with ESR. A possible procedure for the examination of this defect would be to irradiate the crystal at room temperature to produce only F centers (and aggregates), then to cool the crystal to 77 K or lower to observe the spectra. In this way, no other defects would occur which would cover the spectrum, and the unique local symmetry of the tetragonal phase would be imposed on the defect. The spectrum would probably be faint, however.

Further optical study could be done on the F center, as well, such as the polarization of the 400 nm band. Does the polarized bleaching of one type of F center affect the population of the other type? Excitation lifetime studies could indicate the extent to which the F center is localized and how much effect the thermal phonons have on it. ENDOR could also be used to obtain this information.

Optical studies could also be done on the H center. Can the 320 nm band be only partially bleached, as would be the case if it were due to both the H and $V_K$ centers?

H centers in other materials need to be studied. Does the H center exist in $RbMgF_3$ and if it does, what is its

construction? How many fluorines are involved? Does it display the same restricted motion as the $H_A$ center in $KMgF_3$?

$KCaF_3$ has been studied very little beyond its crystal structure. It has similarities to both $KMgF_3$ and $RbCaF_3$. Does it go through phase changes? What are the defects produced by radiation? What are their models? What is the effect of its lattice spacing which is intermediate to $KMgF_3$ and $RbCaF_3$?

The subject of radiation-induced defects in halide materials has been well studied in the past, but there are many more questions such as the extent to which the replacement-collision sequence plays a part in the H center production in halide materials. Can the "area of influence" of the H center defect be described quantitatively to predict the amount of influence of next-nearest anion neighbors? What causes some defects to be preferrentially aligned? What is the structure of these materials following their phase change, and what are the characteristics and effects of the phase changes?

The answers to these questions and many more are needed to fully understand simple crystals and the effect radiation has on them.

## SELECTED BIBLIOGRAPHY


(1) Sonder, E., and W. A. Sibley, "Defect Creation by Radiation in Polar Crystals." Point Defects in Solids, Volume I, General and Ionic Crystals. J. H. Crawford, Jr., and L. M. Slifkin, eds. New York: Plenum Press, pp. 201-283 (1972).

(2) Castner, T. G., and W. Kanzig, J. Phys. Chem. Solids 3, 178 (1957).

(3) Kanzig, W. and T. O. Woodruff, J. Phys. Chem. Solids 9, 70 (1958).

(4) Rose, B. H., J. E. Rhoads, and L. E. Halliburton, Phys. Rev. B 14, 3583 (1976).

(5) Sibley, W. A., and Y. Chen, Phys. Rev. 160, 712 (1967).

(6) Riley, C. R., and W. A. Sibley, Phys. Rev. B 1, 2789 (1970).

(7) Wyckoff, R. W. G., Crystal Structures, 2nd ed., John Wiley and Sons, New York, New York, Copyright, 1964.

(8) Ho, J. C., and W. P. Unruh, Phys. Rev. B 13, 447 (1976).

(9) Bates, J. B., R. W. Major, and F. A. Modine, Solid State Com. 18, 1347 (1976).

(10) Halliburton, L. E., and E. Sonder, Solid State Com. 21, 445 (1977).

(11) Modine, F. A., E. Sonder, and W. P. Unruh, Phys. Rev. B 10, 1623 (1974).

(12) Seretlo, J. R., J. J. Martin, and E. Sonder, Phys. Rev. B 14, 5404 (1976).

(13) Young, M. A., Ph. D. Thesis (Oklahoma State University, 1976).

(14) Koumvakalis, N., and W. A. Sibley, Phys. Rev. B 13, 4509 (1976).

(15) Saha, K. (Private Communication,Oklahoma State University, 1978).

(16) Rhoads, J. E., B. H. Rose, and L. E. Halliburton, Phys. Rev. B 11, 5115 (1975).

(17) Hall, T. E. P., Brit. J. Appl. Phys. 17, 1011 (1966).

(18) Sibley, W. A. (Private Communication,Oklahoma State University, 1978).

(19) Rhoads, J. E., Ph. D. Thesis (Oklahoma State University, 1974).

# APPENDIX

## PROGRAM FLOWCHARTS

### Line Position Prediction Program

This program produces the field values of the electron resonances for several orientations of the magnetic field, similar to an angular dependence study. Rough plotting routines were also available for plotting the calculations, but these are not shown here.

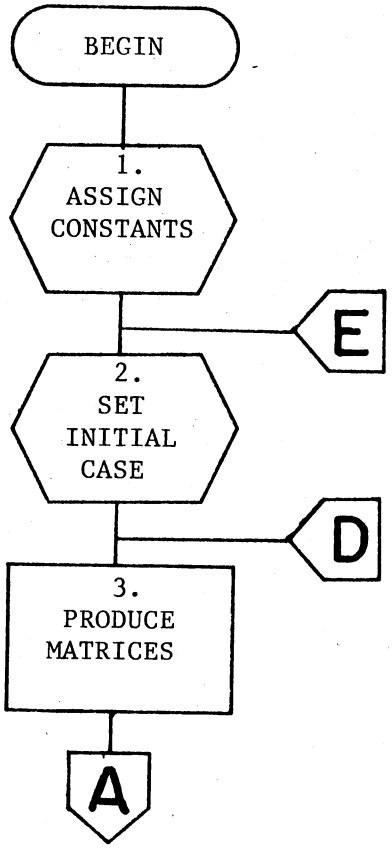


1. Assign the initial constants, such as the Hamiltonian parameters and the initial magnetic field angle.

2. Set the initial case for the model, i. e. the orientation of the defect with respect to the crystal axes. For the case of a [100] defect with gx=gy and Ax=Ay, there are 3 cases.

3. Produce the rotation matrices, which rotate the individual principle axis systems into the magnetic field system.

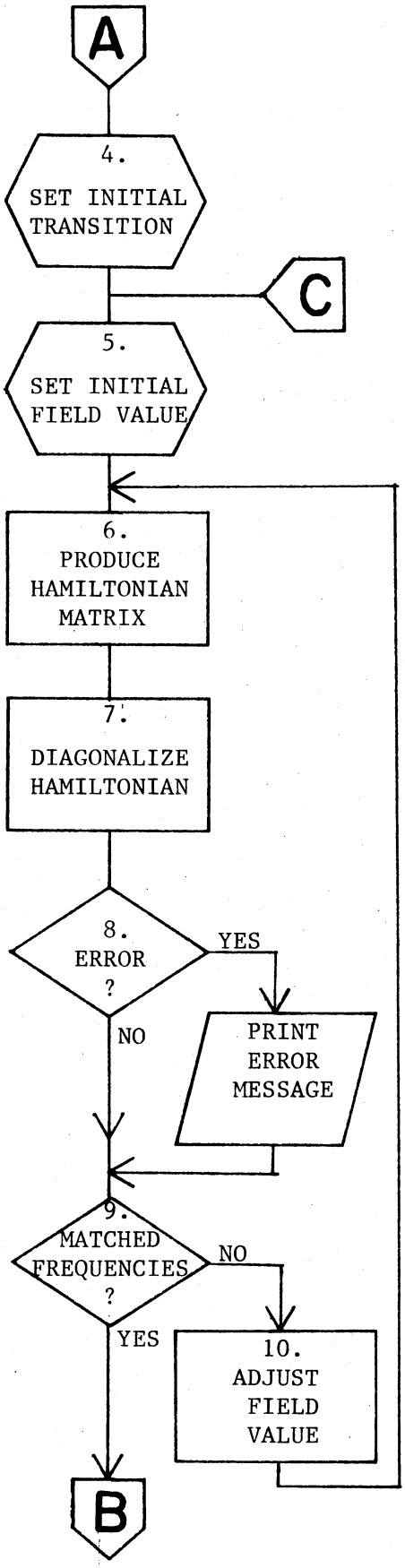


4. Set the initial transition number. Each line in the spectrum is the result of a transition, so that this counts the lines. For an 8X8 Hamiltonian matrix, there are four transitions.

5. Set the initial magnetic field value to some arbitrary number--3,000 Gauss in this case.

6. Produce the Hamiltonian matrix, such that the eigenvalues obtained will be in MHz units.

7. Diagonalize the Hamiltonian matrix and find the eigenvalues. This is done with two subroutines from the EISPACK eigenvalue subroutine package. Diagonalization leaves the eigenvalues in ascending order in a one-dimensional matrix.

8. If an error was flagged in the subroutines, print an appropriate error message (this never occurred).

9. By subtracting the appropriate elements of the eigenvalue matrix, determine if the predicted microwave frequency matches the experimental frequency. If it doesn't, go to 10. If it does, go to 11.

10. Adjust the magnetic field value by multiplying it by the ratio of the experimental to the predicted frequency.

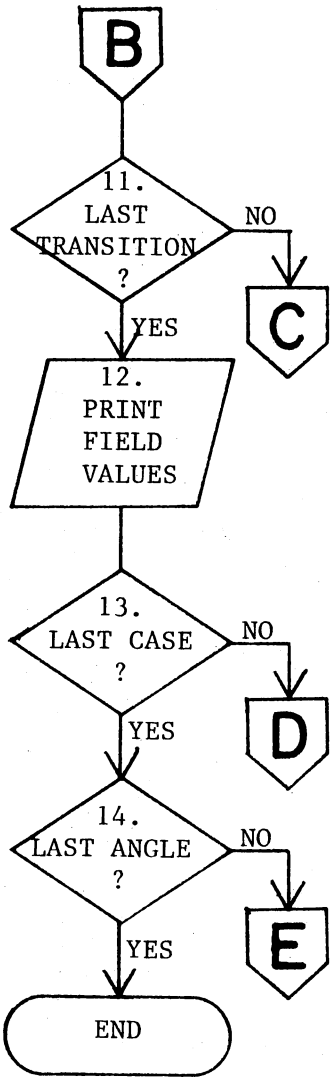


11. If there are any more transiticns, get the next one and go to 5.

12. Print the field values for all transitions for the present field angle and orientation case.

13. If there are more cases, get the next one and go tc 3.

14. If there are more field angles, get the next one and gc to 2. Otherwise, end the program.

## Parameter Fitting Program

This program fit a spin Hamiltonian to the experimental data through recursive adjustment of the g and A parameters and diagonalization of the representative Hamiltonian matrix. Two modified subroutines obtained from J. E. Rhoads' dissertation controlled the process of varying the parameters. These routines were intended to search for a minimum of a function by varying any number of parameters to the function. The function minimized in this case was the sum of the squares of the differences between the field values and angles. See Chapter III for an explanation of the experimental data used.

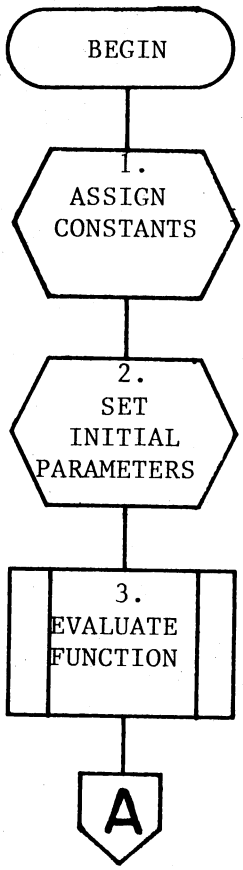


1. Assign the constants used in the program, such as the number of parameters to adjust and the adjustment size.

2. Set the initial parameter values.

3. Evaluate the sum of the squares of the differences between experimental and calculated frequencies for the initial parameters. Save the value. See the next section of this appendix for a flowchart of the function.

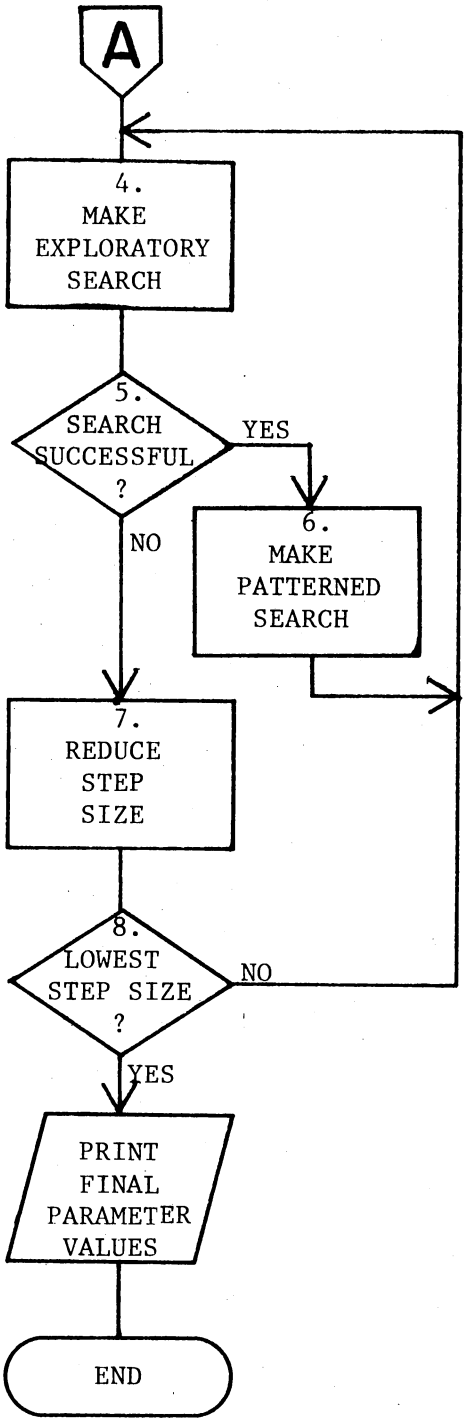


4. Make an exploratory search of each of the parameters in turn by adjusting them up and down, testing if the function value is lowered. Leave each parameter at the value which lowered the function value, or at the original value if the function value was not lowered by the adjustments.

5. Did the search lower the function value? If not, go to 7. If so, go to 6.

6. Make a search, patterned after the results of the previous exploratory search. I. e., if a particular parameter was changed in the exploratory search, change it by the same amount and in the same direction as before until the function value has been minimized. All parameters are adjusted before each evaluation of the function.

7. Reduce the step size by a user defined amount. The step and step reduction sizes are set and kept individually for each parameter.

8. Has the step size been lowerd past its lowest value as set by the user? If not, go to 4 for another exploratory search. If so, write the final parameter values and end the program.

## Function Subprogram to the Parameter Fitting Program

This subroutine calculates the sum of the squares of the differences in experimental and theoretical resonance frequencies for a given set of parameters for the H center in RbCaF . Its resultant answer is minimized by the parameter fitting program to obtain the spin Hamiltonian parameters for the center.

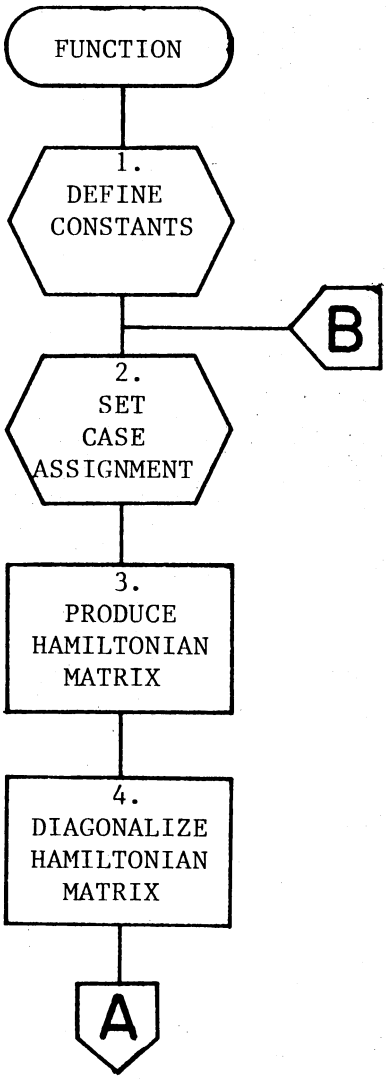


1. Define all needed constants such as the microwave frequency and the experimental magnetic field values. The spin Hamiltonian parameters are passed to the function as parameters in the function call.

2. Set certain indicators for the calculation of a prediction of the line position. This includes selecting the experimental field value, the suspected corresponding orientation, and the particular transition that produces the line.

3. Produce the representative Hamiltonian matrix using the experimental field values and trial parameters.

4. Diagonalize the Hamiltonian and obtain the predicted microwave frequency which would give rise to the transition.

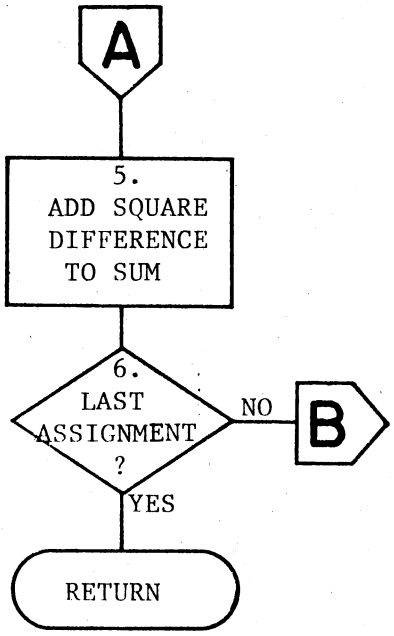


5. Add the square of the difference in predicted and experimental microwave frequencies to the sum of other such squares.

6. Is this the last assignment of an experimental field value to the model? If not, go back to 2 to obtain the next assignment. If so, assign the sum of squares to the function result and return to the calling program.

# VITA[2]

Rick Alan Burris

Candidate for the Degree of

Master of Science

Thesis: ELECTRON SPIN RESONANCE STUDY OF H CENTERS IN $RbCaF_3$

Major Field: Physics

Biographical:

Personal data: Born in Wewoka, Oklahoma, February 10, 1954, the son of Donald Ray and Nancy Sue Burris.

Education: Graduated from Tulsa Memorial High School, Tulsa, Oklahoma, in May, 1972; attended East Central University, Ada, Oklahoma, until December, 1974; attended University of Texas at Arlington, Arlington, Texas, in the summer of 1975; obtained Bachelor of Science degree in May, 1976, from Oklahoma State University; enrolled in the master program at Oklahoma State University in June, 1976. Completed requirements for Master of Science degree in May, 1978.